University of Kent

Kent Academic Repository

Schlichtner, Stephanie, Yasinska, Inna M., Klenova, Elena, Abooali, Maryam, Lall, Gurprit S., Berger, Steffen M., Ruggiero, Sabrina, Cholewa, Dietmar, Milošević, Milan, Gibbs, Bernhard F. and others (2023) *L-Kynurenine participates in cancer immune evasion by downregulating hypoxic signaling in T lymphocytes.* Oncoimmunology 12 . ISSN 2162-4011.

Downloaded from

https://kar.kent.ac.uk/115332/ The University of Kent's Academic Repository KAR

The version of record is available from

https://doi.org/10.1080/2162402X.2023.2244330

This document version

Publisher pdf

DOI for this version

Licence for this version

CC BY-NC (Attribution-NonCommercial)

Additional information

Versions of research works

Versions of Record

If this version is the version of record, it is the same as the published version available on the publisher's web site. Cite as the published version.

Author Accepted Manuscripts

If this document is identified as the Author Accepted Manuscript it is the version after peer review but before type setting, copy editing or publisher branding. Cite as Surname, Initial. (Year) 'Title of article'. To be published in ***Title of Journal*** , Volume and issue numbers [peer-reviewed accepted version]. Available at: DOI or URL (Accessed: date).

Enquiries

If you have questions about this document contact ResearchSupport@kent.ac.uk. Please include the URL of the record in KAR. If you believe that your, or a third party's rights have been compromised through this document please see our Take Down policy (available from https://www.kent.ac.uk/guides/kar-the-kent-academic-repository#policies).

OncoImmunology

ISSN: 2162-402X (Online) Journal homepage: www.tandfonline.com/journals/koni20

L-Kynurenine participates in cancer immune evasion by downregulating hypoxic signaling in T lymphocytes

Stephanie Schlichtner, Inna M. Yasinska, Elena Klenova, Maryam Abooali, Gurprit S. Lall, Steffen M. Berger, Sabrina Ruggiero, Dietmar Cholewa, Milan Milošević, Bernhard F. Gibbs, Elizaveta Fasler-Kan & Vadim V. Sumbayev

To cite this article: Stephanie Schlichtner, Inna M. Yasinska, Elena Klenova, Maryam Abooali, Gurprit S. Lall, Steffen M. Berger, Sabrina Ruggiero, Dietmar Cholewa, Milan Milošević, Bernhard F. Gibbs, Elizaveta Fasler-Kan & Vadim V. Sumbayev (2023) L-Kynurenine participates in cancer immune evasion by downregulating hypoxic signaling in T lymphocytes, OncoImmunology, 12:1, 2244330, DOI: 10.1080/2162402X.2023.2244330

To link to this article: https://doi.org/10.1080/2162402X.2023.2244330

© 2023 The Author(s). Published with license by Taylor & Francis Group, LLC.

View supplementary material

Published online: 10 Aug 2023.

Submit your article to this journal

Article views: 3935

View related articles

View Crossmark data

Citing articles: 29 View citing articles

Full Terms & Conditions of access and use can be found at
https://www.tandfonline.com/action/journalInformation?journalCode=koni20

ONCOIMMUNOLOGY
2023, VOL. 12, NO. 1, 2244330
https://doi.org/10.1080/2162402X.2023.2244330

Taylor & Francis
Taylor & Francis Group

ORIGINAL RESEARCH

OPEN ACCESS Check for updates

L-Kynurenine participates in cancer immune evasion by downregulating hypoxic signaling in T lymphocytes

Stephanie Schlichtner[a,b,c,d], Inna M. Yasinska[a], Elena Klenova[e], Maryam Abooali[a], Gurprit S. Lall[a], Steffen M. Berger[f], Sabrina Ruggiero[f,g], Dietmar Cholewa[f], Milan Milošević[f], Bernhard F. Gibbs[a,g], Elizaveta Fasler-Kan[f], and Vadim V. Sumbayev[a]

[a]Medway School of Pharmacy, Universities of Kent and Greenwich, Chatham Maritime, UK; [b]Department of Personalized Medical Oncology, DKFZ-Hector Cancer Institute at the University Medical Center Mannheim, Mannheim, Germany; [c]Division of Personalized Medical Oncology (A420), German Cancer Research Center (DKFZ); German Center for Lung Research (DZL), Heidelberg, Germany; [d]Department of Personalized Oncology, University Hospital Mannheim, Mannheim, Germany; [e]School of Biological Sciences, University of Essex, Colchester, UK; [f]Department of Pediatric Surgery, Children's Hospital, Inselspital Bern, University of Bern and Department of Biomedical Research, University of Bern, Bern, Switzerland; [g]Department of Human Medicine, University of Oldenburg, Oldenburg, Germany

ABSTRACT

Malignant tumors often escape anticancer immune surveillance by suppressing the cytotoxic functions of T lymphocytes. While many of these immune evasion networks include checkpoint proteins, small molecular weight compounds, such as the amino acid L-kynurenine (LKU), could also substantially contribute to the suppression of anti-cancer immunity. However, the biochemical mechanisms underlying the suppressive effects of LKU on T-cells remain unclear. Here, we report for the first time that LKU suppresses T cell function as an aryl hydrocarbon receptor (AhR) ligand. The presence of LKU in T cells is associated with AhR activation, which results in competition between AhR and hypoxia-inducible factor 1 alpha (HIF-1α) for the AhR nuclear translocator, ARNT, leading to T cell exhaustion. The expression of indoleamine 2,3-dioxygenase 1 (IDO1, the enzyme that leads to LKU generation) is induced by the TGF-β-Smad-3 pathway. We also show that IDO-negative cancers utilize an alternative route for LKU production *via* the endogenous inflammatory mediator, the high mobility group box 1 (HMGB-1)-interferon-gamma (IFN-γ) axis. In addition, other IDO-negative tumors (like T-cell lymphomas) trigger IDO1 activation in eosinophils present in the tumor microenvironment (TME). These mechanisms suppress cytotoxic T cell function, and thus support the tumor immune evasion machinery.

ARTICLE HISTORY
Received 27 April 2023
Revised 23 June 2023
Accepted 31 July 2023

KEYWORDS
cancer; immune checkpoints; immune escape; kynurenine; T cells

Introduction

Immune evasion pathways operated by malignant tumors suppress the function of T lymphocytes and natural killer (NK) cells, which can otherwise attack and kill cancer cells[1]). These pathways mostly include immune checkpoint proteins, along with biochemical pathways that control their expression and functionalization[2]. These networks include programmed cell death protein (PD-1)/programmed death ligand (PD-L1), Tim-3 (T-cell immunoglobulin and mucin domain-containing protein 3)/galectin-9, and V-domain immunoglobulin suppressor of T cell activation (VISTA), as well as signaling cascades regulating immunomodulatory cytokines and growth factors such as transforming growth factor beta type 1 (TGF-β)-Smad-3 and interferon beta or gamma (IFN-β or IFN-γ) pathways[3–6].

However, recent evidence has demonstrated that certain small molecular weight compounds can also effectively suppress T cell function and thus support the evasion of anti-cancer immunity[7,8].

Recently, concerns have been raised regarding the role of L-kynurenine (LKU) and its metabolites in suppressing cytotoxic lymphoid cell function during cancer progression. LKU is an amino acid that is formed during L-tryptophan (L-Trp) catabolism. LKU and its metabolites are formed *via* the kynurenine pathway (KP)[7,8]. KP accounts for approximately 95% of dietary L-tryptophan degradation. Under normal physiological conditions *ca*. 90% of LKU is generated by the hepatic KP[9,10]. In the case of immune activation, the extrahepatic KP plays a more active role. The KP is rate-limited by its first enzyme, Trp 2,3-dioxygenase (TDO), mainly in the liver, and indoleamine 2,3-dioxygenases 1 and 2 (IDO1 and IDO2) elsewhere. IDO1 has been reported to display higher activity than IDO2[9–11]. The entire KP is presented in Supplementary figure S1.[9–12]

Depletion of L-Trp and an increase in LKU exert important immunosuppressive effects by suppressing both T and NK cell functions[9–13]. However, the mechanisms underlying the ability of LKU and its metabolites to suppress lymphoid

CONTACT Vadim V. Sumbayev V.Sumbayev@kent.ac.uk Medway School of Pharmacy, Universities of Kent and Greenwich, Chatham Maritime, UK; Elizaveta Fasler-Kan elizaveta.fasler@insel.ch Department of Pediatric Surgery, Children's Hospital, Inselspital Bern, University of Bern and Department of Biomedical Research, University of Bern, Bern, Switzerland; Bernhard F. Gibbs bernhard.gibbs@uni-oldenburg.de Department of Human Medicine, University of Oldenburg, Oldenburg, Germany

Supplemental data for this article can be accessed online at https://doi.org/10.1080/2162402X.2023.2244330.

© 2023 The Author(s). Published with license by Taylor & Francis Group, LLC.
This is an Open Access article distributed under the terms of the Creative Commons Attribution-NonCommercial License (http://creativecommons.org/licenses/by-nc/4.0/), which permits unrestricted non-commercial use, distribution, and reproduction in any medium, provided the original work is properly cited. The terms on which this article has been published allow the posting of the Accepted Manuscript in a repository by the author(s) or with their consent.

cell function are not clear. One of the possibilities previously discussed is that the depletion of L-Trp is required for the function of these cells[7,8]. However, tryptophan is not necessarily depleted when LKU levels are elevated, and LKU appears to be directly involved in immunological tolerance[7,8]. LKU has also been found to be an aryl hydrocarbon receptor (AhR) ligand[8], however, to date, no direct link has been identified between LKU-AhR interactions and the suppression of T cell function. Importantly, the sources of IDO and LKU are unclear, although their levels are often elevated in the blood plasma of cancer patients as well as in the TME[10]. In some cases, cancer cells express IDOs (mainly IDO1) or even TDO. LKU levels can also be elevated in IDO1-negative cancers[10]. Therefore, we aimed to elucidate the biochemical mechanisms underlying the suppression of T cell function by LKU and to identify the possible sources of LKU in IDO-negative cancers.

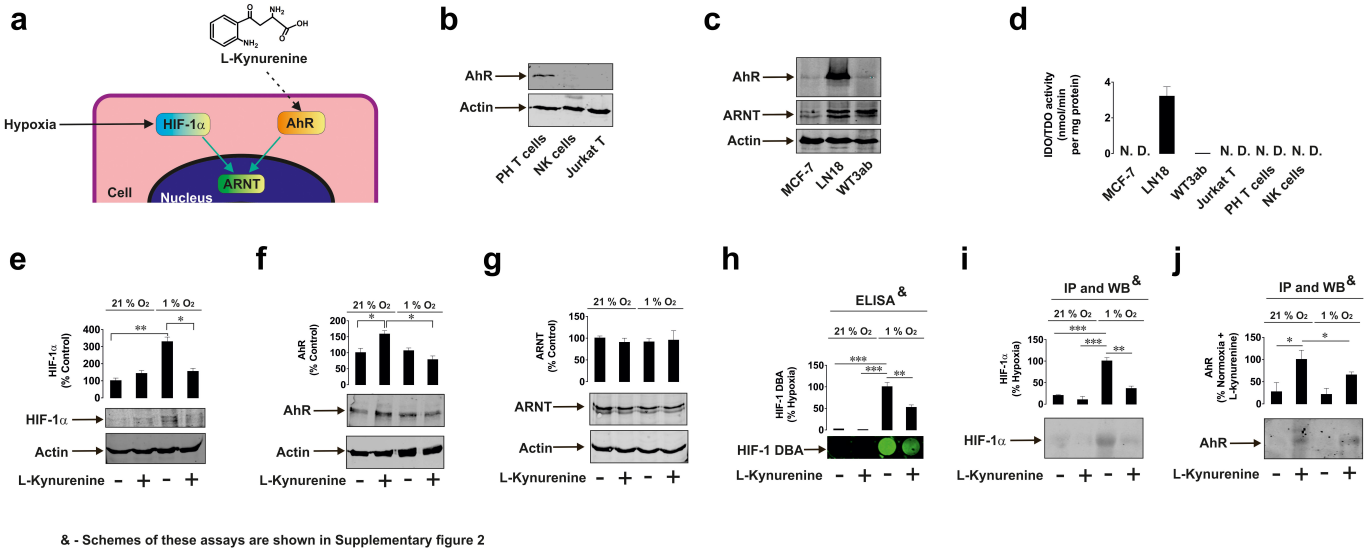
We discovered that LKU suppresses the function of T cells, which either enter hypoxic TMEs or interact with tumor cells, as an AhR ligand. The adaptation of T cells to a hypoxic TME and their interaction with cancer cells require the activation of hypoxia-inducible factor 1 alpha (HIF-1α), which forms the HIF-1 transcription complex with its beta subunit (HIF-1β), also known as the AhR nuclear translocator (ARNT[14]). The presence of LKU in T cells leads to AhR activation, resulting in competition between AhR and HIF-1α for ARNT, which leads to T cell exhaustion. We confirmed that IDO1 expression is induced by interferon–gamma (IFN-γ), but we also discovered for the first time that it is inducible by the TGF-β-Smad-3 pathway. We found that IDO-negative cancers (e. g. breast cancers) still trigger LKU production by activating it elsewhere through the endogenous inflammatory mediator high mobility group box 1 (HMGB-1)-IFN-γ axis. Alternatively, other IDO-negative tumors (e.g., T-cell lymphoma) trigger IDO1 activation in eosinophils, which are present in the TME. All these events lead to elevated LKU levels, allowing for the suppression of cytotoxic lymphoid cell function, thus supporting immune evasion by malignant tumors.

Results

LKU triggers competition between AhR and HIF-1α for ARNT in cells under hypoxic conditions

First, we studied the possible competition between LKU-activated AhR and HIF-1α for ARNT in cells under low-oxygen conditions (Figure 1a). Primary human CD3-positive T cells expressed AhR (Figure 1b). NK cells did not show detectable amounts of AhR by Western blotting, and interestingly, cancerous T cells (Jurkat T) also lacked AhR protein expression (Figure 1b). TDO-positive cancer cells (LN18 high-grade glioblastoma cells), where IDO1 expression can also be induced[15,16], expressed very high levels of AhR and ARNT (Figure 1c), as well as high IDO/TDO activity (Figure 1d). Cells that did not display any IDO activity (MCF-7 human breast cancer cells, WT-3ab Wilms' tumor cells) expressed AhR levels similar to those in primary human T cells and only moderate levels of ARNT.

To identify if there is a competition between AhR and HIF-1α in principle, we used MCF-7 human breast cancer cells and exposed them for 4 h to 50 μM LKU either under normal (21%) or low (1%) oxygen availability. We then obtained nuclear extracts and measured HIF-1α, AhR, and ARNT levels by western blotting. We found that hypoxia upregulated the levels of HIF-1α in the nuclear extracts, which were downregulated by LKU (Figure 1e). Conversely, LKU upregulated AhR levels



& - Schemes of these assays are shown in Supplementary figure 2

Figure 1. LKU induces competition between HIF-1α and AhR for the nuclear translocator. (a) We investigated whether LKU could induce a competition between AhR and HIF-1α for ARNT. (b) AhR levels were compared in primary human CD3-positive T cells, primary human NK cells and Jurkat T cells by Western blot analysis. (c) Expression levels of AhR and ARNT were compared in various cancer cell lines including MCF-7, LN18 and WT3ab. (d) IDO/TDO activity was measured as outlined in Materials and Methods in the cell lines and primary cells described above. (e) MCF-7 cells were exposed to 50 μM LKU under normal (21%) and low (1%) oxygen availability. HIF-1α protein levels, as well as levels of AhR (f) and ARNT (g) were measured in nuclear extracts by Western blot analysis. HIF-1 DNA-binding activity was also analyzed using ELISA-based approach (h). ARNT was immunoprecipitated and proteins bound to it were extracted as outlined in Materials and Methods followed by Western blot detection of HIF-1α (i) and AhR (j). Images are from one experiment representative of four which gave similar results. Quantitative data are shown as mean values ± SEM of four independent experiments. *$p < 0.05$ and **$p < 0.01$ between indicated events.

in the nucleus, whereas this effect was suppressed under low oxygen availability (Figure 1f). The levels of ARNT remained constant regardless of the treatment which the cells underwent.

To directly test if LKU, as such, affects interactions between HIF-1α and HIF-1β we treated MCF-7 cells with 50 μM LKU for 4 h under normal (21%) or low (1%) oxygen availability. This was followed by measuring HIF-1 DNA-binding activity and analyzing the interactions of HIF-1α and AhR with ARNT (HIF-1β) as outlined in Materials and Methods (schemes of these assays are shown in Supplementary figure S2A and B). We found that the presence of LKU significantly reduced HIF-1 DNA-binding activity under hypoxia (Figure 1h). Immunoprecipitation of ARNT followed by extraction of proteins bound to it and their detection by Western blot analysis showed that the presence of LKU significantly reduced the amount of HIF-1α interacting with ARNT (HIF-1β) under low oxygen availability (Figure 1i). Furthermore, hypoxia significantly reduced the amount of AhR bound to ARNT compared to the level observed under normal oxygen availability (Figure 1j). This confirmed our hypothesis that LKU-induced activation of AhR leads to a reduction in the amount of active HIF-1 transcription complex (HIF-1α-ARNT (HIF-1β)).

We then studied whether LKU enters different cell types depending on whether they express IDO1 (Figure 2a). We exposed LN18 human glioblastoma cells (TDO-positive, IDO1 activity inducible) and WT-3ab cells (TDO/IDO1 negative) to 50 μM LKU for 4 h and studied the intracellular LKU levels. We found that they were highly increased in WT-3ab cells and non-significantly increased in LN18 cells (Figure 2b), suggesting that extracellular LKU can enter cells, especially those that do not produce it. Next, we exposed Jurkat T cells (AhR-negative, IDO/TDO-negative), WT-3ab (AhR-positive, IDO-negative), and LN18 cells (AhR-positive, TDO-positive with inducible IDO1 expression) to LKU under low oxygen availability and looked for HIF-1 downstream effects, including intensity of glycolysis and VEGF mRNA levels (both processed are directly controlled by HIF-1[17]; Figure 2c and d). We found that LKU negatively affected glycolysis (Figure 2c) and VEGF mRNA (Figure 2d) levels only in AhR-positive cells (WT-3ab), which at the same time were IDO/TDO-negative. No such effects were observed in AhR-negative Jurkat T-cells. The same results were observed in LN18 cells, which expressed high levels of ARNT and failed to take up extracellular LKU (Figure 2b-d).

IFN-γ and TGF-β induce IDO1 activity and LKU production

Multiple groups have reported that IFN-γ induces IDO1 expression and thus upregulates its activity, whereas TDO expression does not respond to immunological stimulation[16,18]. However, examination of the IDO1 promoter region showed that it has a number of Smad3 response elements. Smad3 activity is induced by TGF-β, which is produced by both cancer cells and T lymphocytes[3]. We therefore investigated whether TGF-β-Smad3 pathways could induce IDO1 expression (Figure 3a).

LN18 cells expressing TDO, where IDO1 expression can be stimulated, were exposed to 2 ng/ml TGF-β for 16 h, followed by the measurement of IDO1 mRNA. We found that it was significantly increased in cells treated with TGF-β (Figure 5b). To verify that Smad3 binds the IDO1 gene directly, we employed ChIP

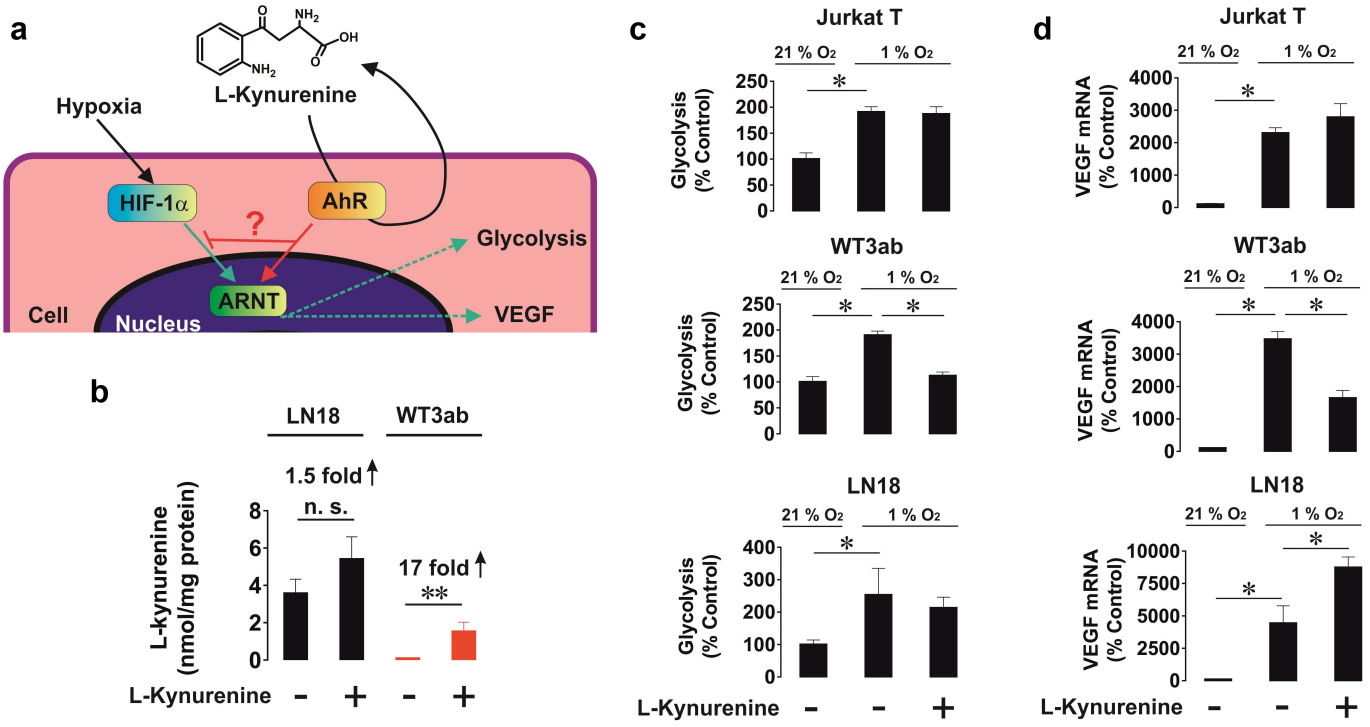


Figure 2. Effects of LKU on HIF-1 activity depends on the cellular expression levels of AhR and ARNT. (a) Cells expressing different levels (LN18 and WT3ab) and not expressing (Jurkat T) AhR were exposed to LKU under low (1%) oxygen availability and the intensity of glycolysis and VEGF mRNA levels were assessed as an indication of HIF-1 responses. (b) LN18 (express TDO and IDO1 expression is inducible) and WT3ab cells (do not express TDO/IDO) were exposed for 4 h to 50 μM LKU and then intracellular LKU levels were measured. Jurkat T cells, WT3ab and LN18 cells were exposed to LKU under low (1%) oxygen availability and the intensity of glycolysis (c) as well as VEGF mRNA levels (d) were measured as outlined in Materials and Methods. Quantitative data are shown as mean values ± SEM of four independent experiments. *$p < 0.05$ and **$p < 0.01$ between indicated events.

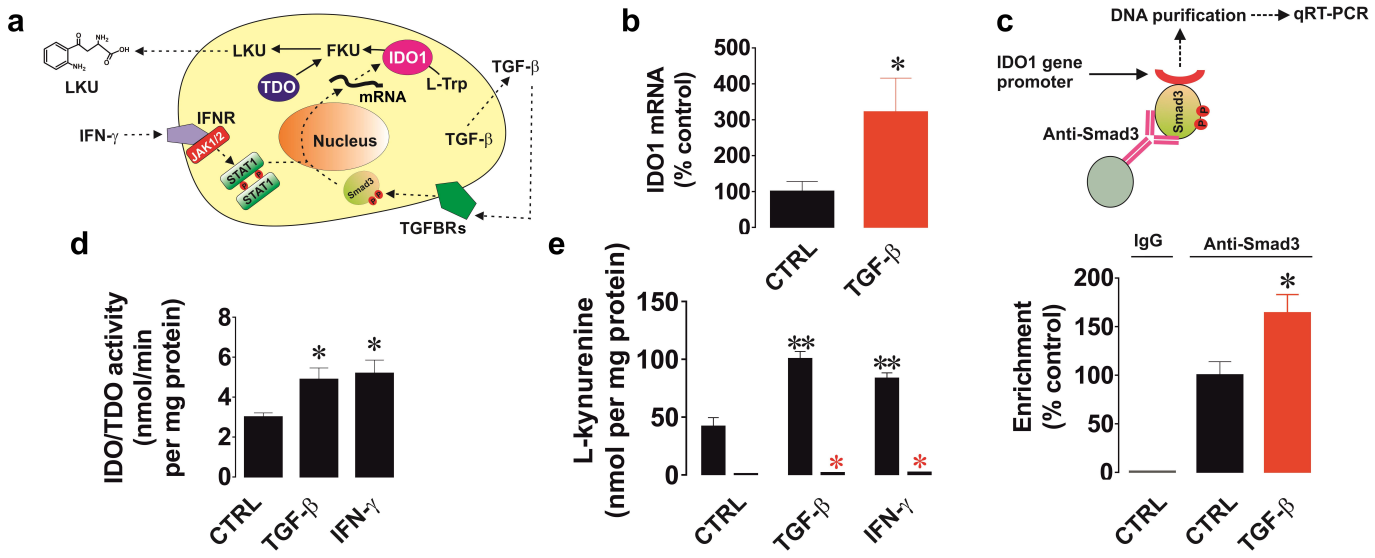


Figure 3. The TGF-β -Smad3 pathway and IFN-γ induce IDO1 expression. (a) We compared the abilities of IFN-γ and TGF-β to induce IDO1 expression in LN18 cells where TDO is expressed at rest and IDO1 expression can be induced. (b) LN18 cells were exposed for 16 h 2 ng/ml TGF-β and then IDO1 mRNA levels were measured using Qrt-PCR as outlined in Materials and Methods. (c) Binding of Smad3 to promoter region of IDO1 gene was measured using ChIP followed by Qrt-PCR in resting LN18 cells and those exposed for 16 h to 2 ng/ml TGF-β. (d) LN18 cells were exposed for 16 h to 2 ng/ml TGF-β or IFN-γ and IDO/TDO was measured in cell lysates. (e) LKU levels were measured in both lysates and conditioned medium of the cells described in the point D of this figure legend. Quantitative data are the mean values ± SEM of four independent experiments. *$p < 0.05$ and **$p < 0.01$ *vs* control.

qRT-PCR using LN18 cells, which confirmed that this process indeed takes place, where TGF-β significantly increased the fold of enrichment (Figure 3c), confirming that Smad3 directly interacts with the promoter region of the IDO1 encoding gene.

Next, we compared the abilities of IFN-γ and TGF-β to induce IDO1 activity in LN18 cells. Cells were exposed to 2 ng/ml IFN-γ or TGF-β for 16 h, and we then investigated IDO1/TDO activity, as well as the levels of cell-associated and released LKU. We found that both TGF-β and IFN-γ significantly upregulated IDO1 activity (Figure 3d) and the levels of released (Figure 3e, left bar in each pair) and cell-associated (Figure 3e, right bar in each pair) LKU. These results confirm that IDO1 activity and LKU production can upregulate both IFN-γ and TGF-β.

LKU downregulates HIF-1 activity in AhR-expressing T lymphocytes

In the next set of experiments, we compared the effects of naturally produced LKU on HIF-1 activity (measured by assessing the quantities of VEGF mRNA[17]) in Jurkat T cells, which lack AhR, and primary CD3-positive human T cells, which express moderate AhR levels.

Jurkat T cells (in suspension) were co-cultured for 16 h at a ratio of 1:1 with LN18 human glioblastoma cells (adherent), which display TDO and inducible IDO1 activity and release LKU, for 16 h. Jurkat T cells were then separated and mRNA was isolated. Upon completion, the coculture conditioned medium contained 42 ± 7 μM LKU. We found that VEGF mRNA levels were highly increased in Jurkat T cells co-cultured with LN18 compared with resting Jurkat T cells (Figure 4a). TGF-β levels in the conditioned medium were also highly increased in the co-culture, which explains the high LKU levels (see above and Figure 4a). We then co-cultured LN18 cells with primary CD3-positive human T cells for 16 h, at a ratio of 1:1, in the absence or presence of 1 μM epacadostat (an IDO1 inhibitor). The level of LKU released in the co-culture was 56 ± 12 μM, which was significantly decreased in the presence of epacadostat (Figure 4b). We then added both IDO1 (epacadostat) and TDO (680C91) inhibitors, which led to a complete attenuation of LKU production, suggesting the presence of both TDO and IDO1 activities (Figure 4b). TGF-β levels (released by cancer cells and which affects T cell functions[19,20]) increased in the presence of LN18 cells and decreased in the presence of IDO1/TDO inhibitors (Figure 4b). Importantly, VEGF mRNA levels remained unchanged in primary T cells co-cultured with LN18 cells compared to those in resting T cells. However, in the presence of epacadostat, VEGF mRNA levels in primary human T cells were significantly upregulated and further increased in the presence of 680C91 (Figure 4b), which clearly showed that HIF-1-dependent VEGF expression in T cells was downregulated by LKU.

We then investigated whether LKU affected the cytotoxic activity of primary human T cells. We co-cultured K562 human chronic myeloid leukemia cells (pre-treated for 24 h with 100 nM PMA) in the wells of a 96 well plate (adherent) with CD-3-positive primary human T cells (in suspension) for 16 h in the absence or presence of 50 μM LKU. As controls, we used non-co-cultured PMA-pretreated K562 cells that were not treated or exposed to 50 μM LKU for 16 h (Figure 5a).

We then measured the levels of TGF-β and IL-2 (as suggested above, released by helper T cells in order to activate cytotoxic T cells[20]) in the conditioned medium. We found that the levels of secreted TGF-β were significantly increased in K562 cells in the presence of LKU. TGF-β levels were very low in the K562–T cell co-culture, but highly increased when these co-cultures were exposed to LKU (Figure 5b).

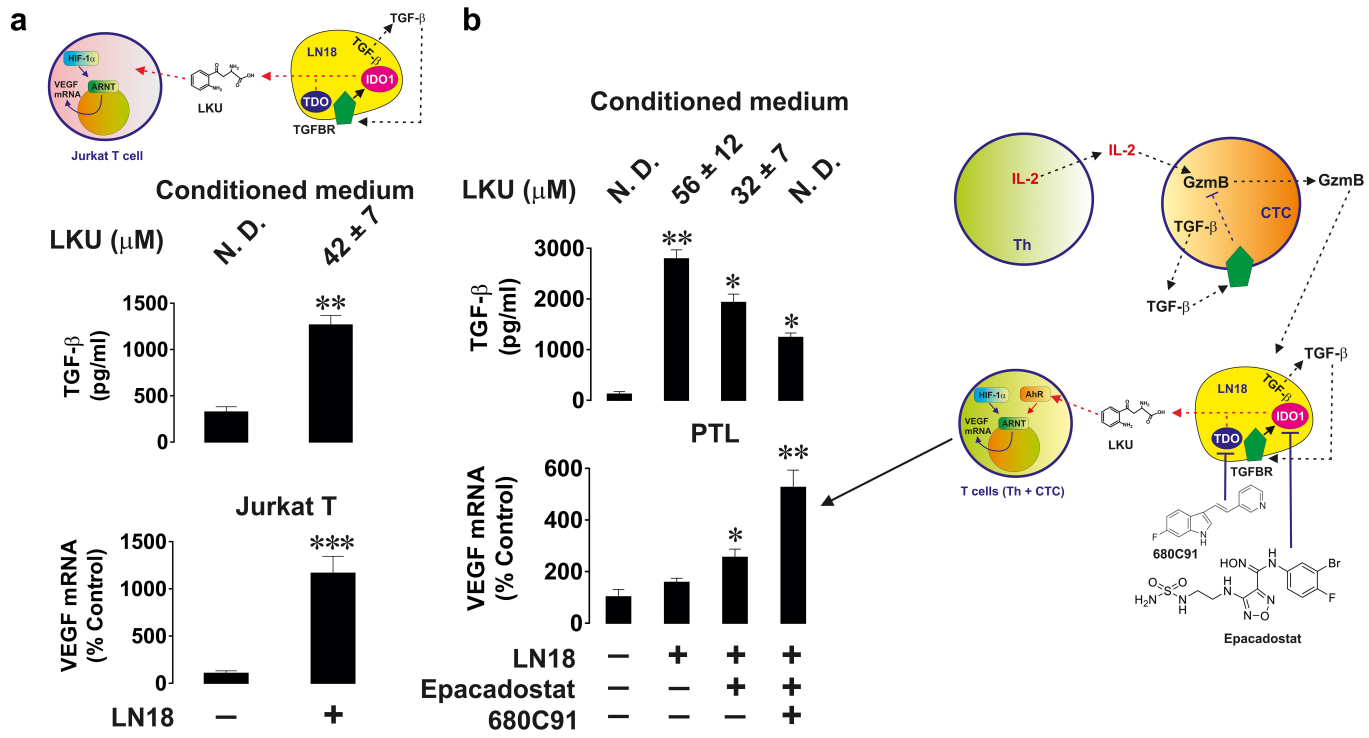


Figure 4. LKU downregulates HIF-1 activity in primary human T cells interacting with cancer cells. (a) Jurkat T cells (which do not express AhR) were co-cultured for 16 h with LN18 cells at a ratio of 1:1. VEGF mRNA levels in Jurkat T cells and TGF-β as well as LKU levels were then measured in the conditioned medium. (b) Primary human CD3-positive T cells (express AhR) were co-cultured for 16 h with LN18 cells at a ratio of 1:1 in the absence or presence of 1 μM epacadostat (IDO1 inhibitor) or combination of 1 μM epacadostat and 1 μM 680C91 (TDO inhibitor). VEGF mRNA levels in T cells and TGF-β as well as LKU levels were then measured in the conditioned medium. Quantitative data are shown as mean values ± SEM of four independent experiments. *$p < 0.05$ and **$p < 0.01$ *vs* control.

IL-2, which is produced by T cells, was undetectable in the conditioned medium after culturing K562 cells regardless of the presence of LKU. However, in co-culture with T cells, IL-2 release was clearly detectable but was downregulated in the presence of LKU (Figure 5c).

The viability of K562 cells was affected by T cells, but was restored in the presence of LKU (Figure 5d). Granzyme B activity in K562 cells was undetectable in the absence of T cells but was clearly detectable in their presence. However, in the presence of LKU, granzyme B activity in K562 cells co-cultured with T cells was significantly lower than that in the absence of LKU (Figure 5e).

LKU levels were undetectable in T cells co-cultured with K562 cells but were high in cells where LKU was present in the medium (Figure 5f). VEGF mRNA levels in T cells co-cultured with K562 cells were downregulated by LKU (Figure 5g), which was in line with the results shown in Figure 5b.

IDO-negative cancers can still lead to high levels of LKU production recruiting other body systems to generate LKU

We investigated five malignant breast tumor samples *versus* healthy breast tissue samples obtained from the same patients during surgery. We found that AhR levels in these tumors were barely detectable by western blotting, and in healthy tissues, it was not detectable at all (Figure 6a). Importantly, neither healthy nor cancerous tissues displayed IDO/TDO activity and did not produce LKU. LN18 cells were used as positive controls. Similarly, all breast cancer cell lines were IDO-negative and were unable to produce detectable amounts of LKU (Figure 6b).

We then compared the blood plasma of 15 healthy donors *versus* 15 samples obtained from patients with primary or metastatic breast cancer (see Materials and Methods for details). We found that patients with primary breast cancer had LKU levels similar to those in healthy donors, while patients with metastatic breast cancer had significantly higher LKU levels in their blood plasma (Figure 6c). The levels of TGF-β in all breast cancer patients were similar to those seen in healthy donors (Figure 6d), whereas IFN-γ levels were significantly upregulated in the blood plasma of metastatic breast cancer patients (Figure 6e). Correlation analysis demonstrated a very high R^2 (0.9399) between IFN-γ and LKU levels in the blood plasma of the patients (Supplementary figure S3). IFN-γ production is normally a result of Toll-like receptor (TLR) 4 activation by exogenous or endogenous ligands. One such ligand is the high-mobility group box 1 (HMGB1) protein, which is produced by stressed or apoptotic cells. Malignant tumors, especially metastatic tumors, normally produce high HMGB1 levels. We therefore measured HMGB1 levels in the blood plasma of the studied patients and found that levels were significantly increased in the blood plasma of metastatic breast cancer patients but not in primary breast cancer patients (Figure 6f). There was also a strong correlation ($R^2 = 0.7382$) between HMGB1 and IFN-γ levels in the blood plasma of these patients (Supplementary figure S3).

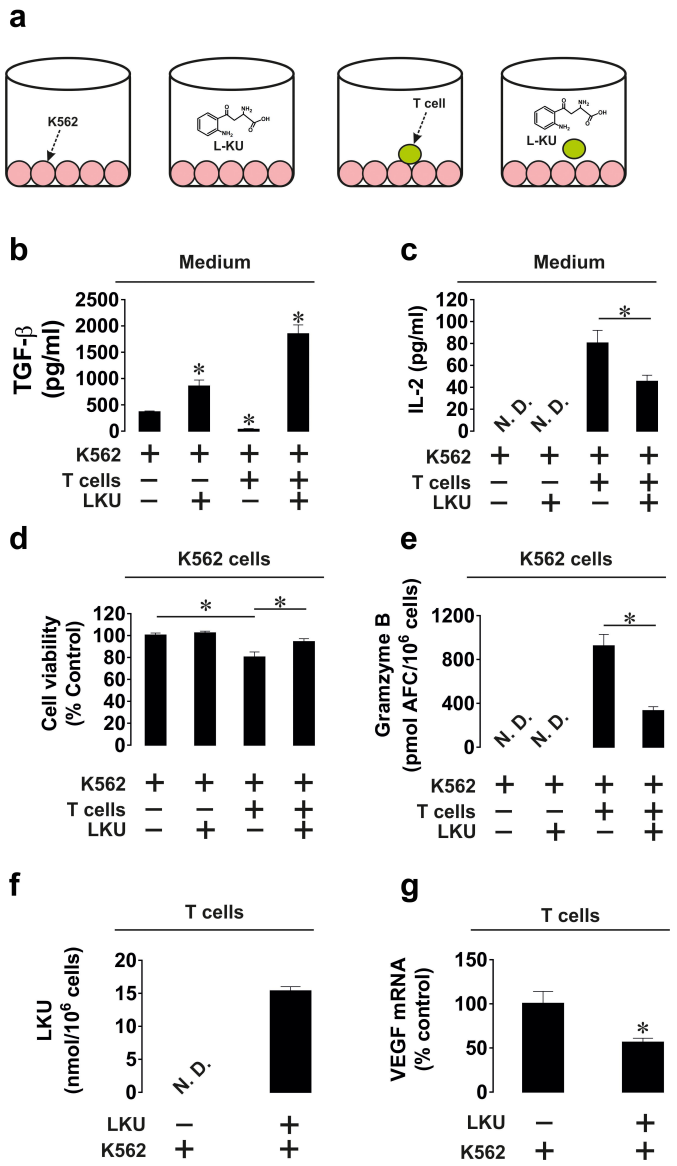


Figure 5. LKU downregulates the ability of primary human T cells to kill cancer cells. (a) PMA-pre-treated K562 cells were co-cultured with CD3 positive primary human T cells for 16 h in the absence or presence of 50 μM LKU. TGF-β (b) and IL-2 (c) levels were measured in the conditioned medium by ELISA. Viability of K562 cells (d) and Granzyme B activity (e) in them was measured as outlined in Materials and Methods. LKU levels (f) and VEGF mRNA levels (as indicator of HIF-1 activity) were measured in T cells. Quantitative data are shown as mean values ± SEM of five independent experiments. *$p < 0.05$ between indicated events.

We confirmed in *ex vivo* models that HMGB1 triggers IFN-γ production in ex vivo models. We isolated primary mononuclear leukocytes from the blood of healthy human donors and exposed these cells to 1 μg/ml HMGB1 for 24 h, maintaining them in RPMI-1640 medium supplemented with fetal bovine serum and penicillin/streptomycin (see Materials and Methods for details). We measured the levels of IFN-γ secreted by these cells and found that these levels were highly increased in the conditioned medium used to culture human cells in the presence of HMGB1 (Supplementary figure S4).

This suggests that, in IDO/TDO-negative cancers such as breast cancer, LKU levels could be upregulated *via* a complex mechanism involving the production of HMGB-1, which then activates IFN-γ secretion. IFNγ is known to induce the expression of extrahepatic IDO1 in tissues[18], which can then convert L-Trp into LKU, thus helping malignant tumors suppress cytotoxic T cells (see Discussion for more details and Figure 7a-c).

Eosinophils present in the tumor microenvironment (TME) participate in tumor-mediated suppression of immune surveillance by producing LKU

We investigated a case of a very rare high-grade T-cell lymphoma non-otherwise specified (HGTCL-NOS) in which the patient had a high level of eosinophils in the TME, as confirmed by histopathology. At diagnosis, the patient had low levels of IL-2 and galectin-9 in the blood plasma but extremely high levels of LKU, VISTA, and TGF-β (Figure 8). Upon successful completion of six cycles of CHOEP chemotherapy (cyclophosphamide, doxorubicin, vincristine, etoposide, and prednisolone), the levels of IL-2 were upregulated, galectin-9 levels were unchanged, and LKU, VISTA, and TGF-β levels returned to those observed in healthy donors (Supplementary figure S5). IFN-γ levels in the patient's blood plasma were barely detectable at all stages when the measurements were completed.

We then tried to model this kind of TME and co-cultured Jurkat T cells (as malignant T cells which express VISTA but do not secrete it at rest or in the presence of TGF-β[2], a growth factor, which can upregulate VISTA expression in these cells) with primary CD-3 positive human T cells and EoL1 human eosinophils (in a ratio of 2:1:1, respectively) (Figure 8a). We observed TGF-β and LKU production as well as the effects of LKU on glycolysis (a HIF-1-dependent process). When glycolysis is required, but not upregulated, cells produce increased levels of methyl glyoxal (MGO[21]). As such, the downregulation of glycolytic degradation of glucose can be assessed by measuring the MGO levels (Figure 8b). These co-cultures were performed in the absence or presence of 1 μM epacadostat. We found that when Jurkat T cells were co-cultured with other cell types, TGF-β levels increased (Figure 8c – and further increased in the presence of epacadostat). VISTA levels were upregulated when Jurkat T cells were present together with primary T cells, regardless of the presence of eosinophil/epacadostat, suggesting that VISTA was released by T cells (most likely Jurkat T cells), although one cannot rule out the contribution of primary T cells (Figure 8c). The levels of IFN-γ were very low and did not significantly change in the various cultures/co-cultures, except in the presence of epacadostat. However, all IFN-γ concentrations observed (unlike those of TGF-β) were too low to induce biological effects (Figure 8c). Granzyme B activity in the medium was stably increased when Jurkat T cells, eosinophils (or both) were co-cultured with primary human T cells (Figure 8d). However, when all three cell types were combined, granzyme B activity in the medium (released granzyme B) was significantly lower and was only restored in the presence of epacadostat (Figure 8d). Interestingly, MGO levels were increased in the medium in which eosinophils were co-cultured with both Jurkat T cells and primary T cells, and this effect was abolished by epacadostat (Figure 8d). LKU levels were upregulated in all cases in

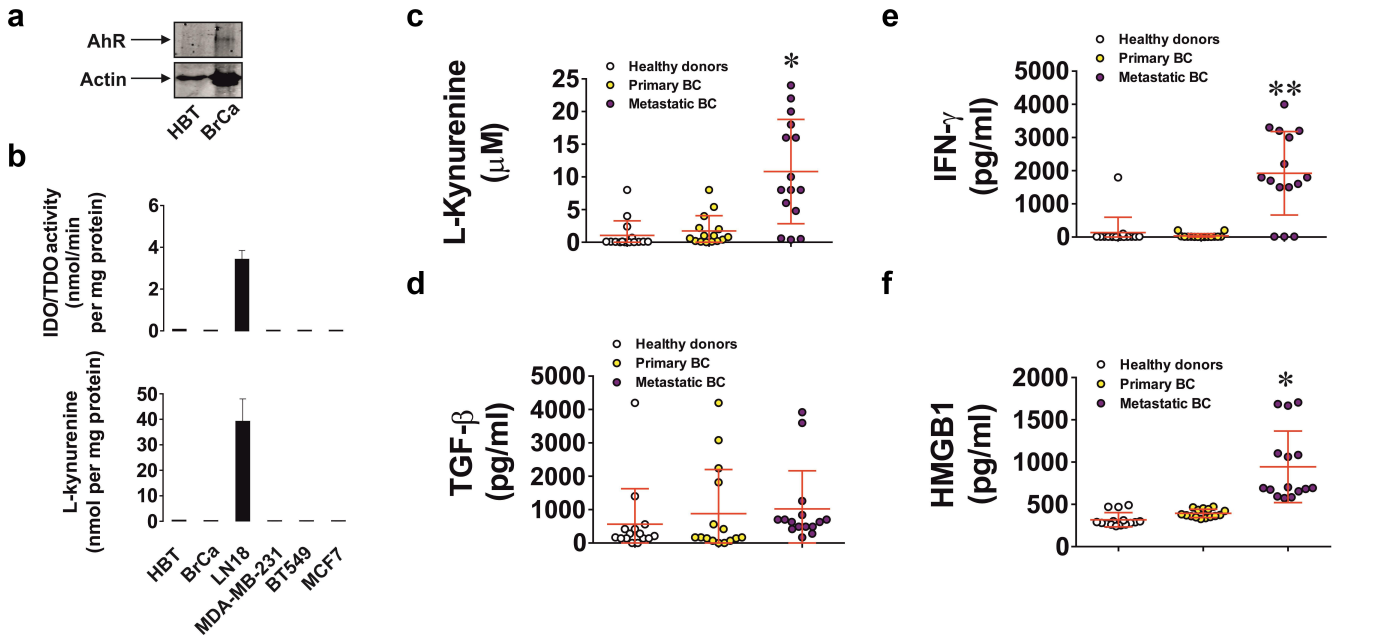


Figure 6. IDO/TDO-negative breast cancer leads to increased blood plasma LKU levels at metastatic stage. (a) Expression of AhR protein was analyzed in primary breast tumors *vs* healthy tissues by Western blot. (b) IDO/TDO activity and LKU levels were assessed in malignant breast tumors and healthy breast tissue homogenates and in various metastatic breast cancer cell lines. The LN18 cell line was used as a positive control. (c) LKU, (d) TGF-β, (e) IFN-γ and (f) HMGB1 levels were assessed in blood plasma from 15 primary breast cancer patients, 15 metastatic breast cancer patients and 15 healthy donors as outlined in Materials and Methods. Quantitative data show mean values ± SEM of five independent experiments for (a) and (b) and 15 independent experiments for (c) – (f). *$p < 0.05$ between indicated events.

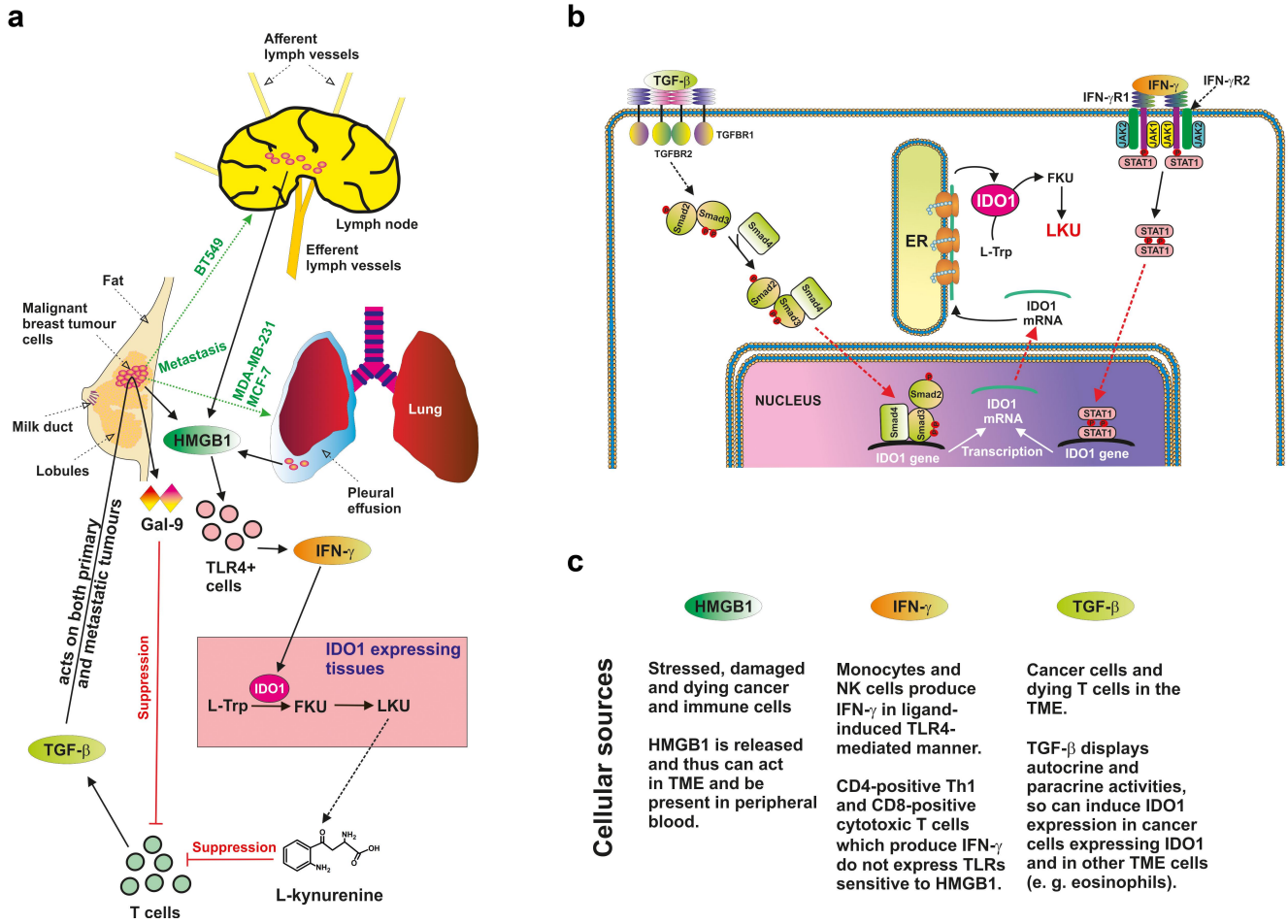


Figure 7. (a) Scheme of the integrative immune evasion machinery. The scheme also shows the origin of the studied cell lines and the possible integration of LKU and galectin-9 into anti-cancer immune escape networks. (b) Involvement of TGF-β-Smad3 and IFN-γ-JAK/STAT pathways in IDO1 expression in human cells. (c) Outline of cellular sources of HMGB1, IFN-γ and TGF-β used in the immune evasion networks described in the section (a).

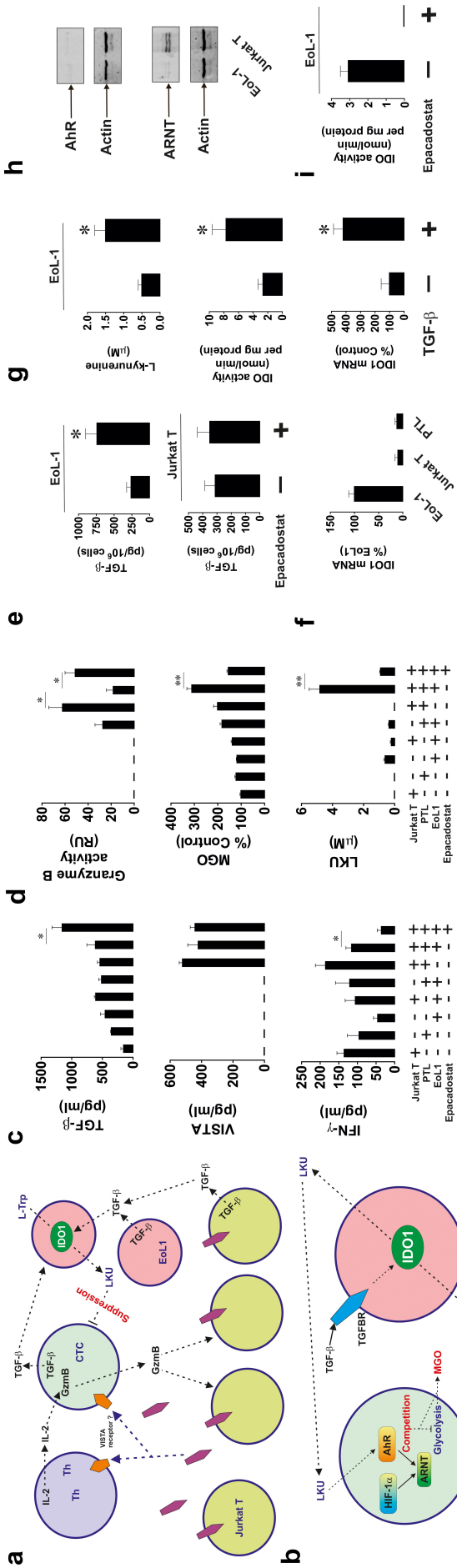


Figure 8. (a) Jurkat T cells (VISTA-producing malignant T cells) were co-cultured with EoL1 eosinophils and primary human CD3-positive T cells at a ratio of 2:1:1 in the absence or presence of epacadostat. (b) TGF-β-dependent upregulation of IDO1 activity and possible LKU effects on primary CD3-positive T cells are highlighted. (c) TGF-β, VISTA and IFN-γ levels were measured my ELISA in the conditioned medium. (d) Granzyme B, MGO and LKU levels were detected as outlined in Materials and Methods. (e) Jurkat T or EoL1 cells were exposed to 1 μM epacadostat for 16 h followed by detection of TGF-β levels in conditioned medium. (f) IDO1 mRNA levels were measured in EoL1, Jurkat T and primary CD3-positive T cells using Qrt-PCR. (g) EoL1 cells were exposed to 2 ng/ml TGF-β for 16 h followed by detection of IDO1 mRNA levels, IDO activity in the cells and LKU levels in the medium. (h) Levels of AhR and ARNT were compared in EoL1 and Jurkat T cells by Western blot analysis. (i) EoL1 cell lysate was used as a preparation of IDO1 and IDO activity was measured in the absence or presence of 1 μM epacadostat. Images are from 1 experiment representative of 4 which gave similar results. Quantitative data are shown as mean values ± SEM from four independent experiments. $*p < 0.05$.

which eosinophils were present. Importantly, they were very high when eosinophils, Jurkat T, and primary T cells were co-cultured and were reduced in the presence of epacadostat (this was in line with reduced granzyme B release, where LKU could have contributed to primary T cell exhaustion (Figure 8d).

We then examined whether epacadostat could induce TGF-β production in eosinophils and Jurkat T cells and found that this was the case for EoL1 cells but not Jurkat T cells (Figure 8e). Interestingly, IDO1 mRNA was present in EoL1 cells, but only traces were detectable in both Jurkat and primary T cells (Figure 8f). IDO1 mRNA levels, IDO activity, and LKU production were clearly detectable and were significantly upregulated by TGF-β (Figure 8g), which is in line with our observations. Importantly, AhR was not detectable in EoL1 or Jurkat T cells (Figure 8h), although EoL1 expressed very low levels of ARNT (Figure 8h). Finally, epacadostat completely attenuated IDO activity in EoL1 cell lysates, confirming its DO-inhibitory properties (Figure 8i).

Taken together, these results suggest that eosinophils present in the TME may react by activating IDO1 and are thus capable of producing LKU, which downregulates the cytotoxic potential of T cells.

Discussion

LKU has been reported to play a crucial role in the immune evasion machinery operated by a wide range of cancers[22]. Normally, LKU is produced mainly in the liver by TDO[9,10]. However, outside the liver LKU is generated by IDO1 in cells such as eosinophils, whereas other cell types may express IDO2[9]. Of these two enzymes, IDO1 is the most active and common. Some malignant tumors are IDO-positive and can generate LKU themselves[22]. For example, this has been reported in pancreatic ductal adenocarcinomas[23]. However, the biochemical mechanisms that control IDO1 activity remain unclear, except for IFN-γ-induced IDO1 expression, which has been confirmed by various research groups[18]. In addition, the mechanisms underlying the ability of LKU to downregulate cytotoxic T-lymphocyte activity are poorly understood. Here, we hypothesized that LKU, as an AhR ligand, induces the translocation of AhR into the nucleus. In an aggressive TME, AhR can then compete with HIF-1α for the ARNT (HIF-1β) (both proteins use the same nuclear translocator).

In this study, we have shown that primary human T cells express moderate levels of AhR and thus respond to LKU in an AhR-dependent manner (Figure 1b). Importantly, we found that human cancer cells that do not express IDO/TDO produce low or moderate amounts of AhR (Figure 1c and d). Conversely, malignant cells that express IDO/TDO and thus produce LKU (e.g., LN18 glioblastoma cells) also express high levels of AhR and, importantly, high levels of ARNT. This most likely covers the needs of both HIF-1α when it is activated, and AhR when its transcriptional activity is induced by a ligand such as LKU. To perform basic biochemical tests, we used MCF-7 human breast cancer cells, which express AhR levels similar to those observed in T cells (Figure 1). We found that LKU reduced nuclear levels (most likely by affecting nuclear translocation) of HIF-1α under low oxygen availability. In contrast, nuclear levels of AhR in the presence of LKU are much higher under normal oxygen availability than under hypoxic conditions. Importantly, the nuclear levels of ARNT remained unchanged in all cases, which supports our conclusion (Figure 1e-g). Furthermore, we directly confirmed that LKU-dependent activation of AhR affects formation of HIF-1 transcription complex under low oxygen availability. Simultaneously, low oxygen availability decreases amounts of the AhR-ARNT complex (Figure 1h-j) suggesting a direct competition between AhR and HIF-1α for ARNT. Interestingly, we found that if cells do not express IDO/TDO, and thus do not convert L-Trp into LKU, they take up much more exogenous LKU than those that display IDO/TDO activities (Figure 2b).

HIF-1 activity in real time can be determined by measuring glycolysis and VEGF mRNA levels[17]. Therefore, it is quite clear that neither glycolysis nor VEGF mRNA levels are affected by LKU under hypoxic conditions in cells that do not express AhR (Jurkat T) or in cells that produce LKU (LN18, Figure 2c and d). However, in cells that express AhR but do not produce LKU, both glycolysis and VEGF mRNA levels were significantly downregulated by exogenous LKU under low oxygen availability (Figure 2c and d). Therefore, it is obvious that the effect depends on AhR/ARNT, and in cells that produce IDO/LKU (LN18), the uptake of exogenous LKU, and thus the increase in its intracellular concentration, is lower than that in cells that do not display natural production of LKU (Figure 2).

Interestingly, only IFN-γ and its downstream pathway are known to induce IDO1 activity and LKU production (TDO expression is not induced by immunological stimulation)[16,18]. We found that the TGF-β-Smad3 pathway was also responsible for upregulating IDO1 expression in cells that naturally produce this enzyme (Figure 3). This is a potentially important finding, since TGF-β levels are increased in the TME, in which cancer cells themselves and affected T cells are a source[19,20].

If cells that naturally produce LKU (LN18, adherent cells) are co-cultured with Jurkat T cells (which do not express AhR) or primary human CD3-positive T cells (which express AhR), the effects on VEGF mRNA levels in these T cells are very different. They are increased in Jurkat T cells and do not change in primary T lymphocytes. However, when primary T cells were co-cultured with LN18 in the presence of 1 μM epacadostat (IDO1 inhibitor), the levels of VEGF mRNA were significantly increased (Figure 4b). If 1 μM 680C91 (a TDO inhibitor) is added to epacadostat, the levels of VEGF mRNA are increased even further (Figure 4b). Importantly, TGF-β levels were highly upregulated in co-culture (especially with primary T cells); however, they were reduced in the presence of epacadostat and 680C91 in proportion to the reduction in LKU levels. Affected T cells are known to release TGF-β[19] and our results shown here suggest that LKU contributes to T cell suppression.

When K562 cells were co-cultured with primary CD3-positive T cells, TGF-β levels were significantly higher in the presence of LKU, and thus T cells were affected (Figure 5b). Therefore, if cancer cells express TDO/IDO, TGF-β further upregulates this expression and LKU production.

LKU was also found to downregulate the ability of primary human T cells to kill K562 chronic myeloid leukemia cells.

K562 cells are an easy target for T and NK cells because they do not operate efficiently in the immune evasion machinery[24]. Exogenous LKU reduced IL-2 production by T helper cells and the levels of granzyme B released by cytotoxic T cells. In addition, killing of K562 cells by T cells was attenuated by LKU. In line with the observations described above, the levels of VEGF mRNA in T cells co-cultured with K562 cells were significantly reduced in the presence of LKU (see Figure 5). These findings confirmed that LKU crucially affects T cell function and is associated with reduced hypoxic signaling, which is required for adaptation to stress. Furthermore, LKU affects the entire T cell machinery involved in anti-cancer immunity.

However, there are some cancers (such as metastatic breast cancer), where high levels of LKU are detected in blood plasma (Figure 6), which do not express IDO/TDO and do not display any enzymatic conversion of L-Trp into LKU. Here, TGF-β levels did not increase, whereas IFN-γ concentrations were significantly upregulated. This correlates with high levels of HMGB1 protein, which could induce IFN-γ production in a toll-like receptor 4 (TLR4)-dependent manner (Figure 6).

We confirmed that HMGB1 induced IFN-γ secretion in human mononuclear leukocytes (Supplementary figure S4). IFN-γ induces IDO1 (but not TDO) expression and thus can trigger an increase in LKU production and blood plasma levels, respectively. Interestingly, when we analyzed individual patients, we observed a clear correlation between blood plasma levels of HMGB1, IFN-γ, and LKU (Supplementary figure S3), supporting the above statements.

Based on our findings, we propose a map of the immune evasion machinery operated by such cancers, such as metastatic breast cancer (Figure 7a). Cells forming tumors, and their associated tissues normally release HMGB1, especially when they are stressed or damaged[5,25,26]. This can also be done by damaged immune cells and other affected nonmalignant cells, and thus must be a common process in metastatic cancers (which is confirmed by our results (Figure 6f)), triggering HMGB1-dependent IFN-γ production (e. g. in TLR4-dependent manner[27]). Ligand-dependent activation of TLR4 induces IFN-γ production by monocytes[28] and NK cells[29]. IFN-γ triggers the upregulation of LKU in IDO1-expressing tissues and thus elevates its blood plasma levels. T cells in the TME are killed by immune checkpoint proteins such for example, galectin-9 (and this killing becomes easier when T cells are affected by LKU). These T cells release TGF-β into the TME, which, together with TGF-β produced by cancer cells, triggers further upregulation of galectin-9 in tumor cells, thus enhancing the strength of the immune evasion machinery (Figure 7a). TGF-β-Smad3 and IFN-γ-JAK/STAT pathways leading to IDO1 expression are shown in the Figure 7b. Cellular sources of HMGB1, IFN-γ and TGF-β are summarized in the Figure 7c.

Another aspect that we explored was how eosinophils, when entering the TME with the purpose of facilitating T cell TME migration, produce LKU, which appears to work in the tumor's favor. We analyzed blood samples from a patient with high-grade T-cell lymphoma (originating from CD4-positive granzyme B-negative T helper cells) not non-otherwise specified (HGTCL-NOS), stage IV, which is a very rare type of cancer. Eosinophils were present in the TME and, in the plasma, the patient had very high levels of soluble VISTA compared to healthy donors, normal levels of galectin-9, and extremely high levels of TGF-β. IFN-γ levels were not detectable, IL-2 levels were low, and LKU levels were high (Supplementary figure S5). Therefore, we suggest that TGF-β may induce IDO1 expression in cells such as eosinophils, which then produce and release LKU. Our partial reconstruction of the TME by co-culturing Jurkat T cells (as malignant T helpers), EoL1 human eosinophils, and primary human T cells supports this, where we observed that LKU levels were increased in the presence of eosinophils. When all described cell types were present, LKU levels were very high, leading to a major reduction in granzyme B release by cytotoxic T cells. Increased MGO levels also indicated that glycolysis was overloaded because of LKU-mediated inhibition of HIF-1α. Furthermore, this effect can support tumor growth since MGO is known to engage in the Maillard reaction. This involves L-lysine in proteins forming an Amadori adduct, which is converted into carboxymethyl lysine and then further converted to advanced glycation end products (AGE). As a result, tumor growth is supported by increased proliferative activity of cancer cells *via* interaction with the receptor of AGE (RAGE) and induction of mitogenic signaling[21]. Epacadostat (an IDO inhibitor) attenuated the effects of LKU described above (Figure 8). Eosinophils, but not any other cells involved in these experiments, expressed IDO1 (Figure 8f), and its activity and LKU production were strongly upregulated by TGF-β in these cells.

Taken together, these results suggest that LKU is capable of suppressing the anticancer activity of T cells. One of the biochemical mechanisms through which this effect is achieved is the interaction of LKU with AhR, leading to the inhibition of HIF-1α nuclear translocation. A lack of adaptation to a stressful environment, which is a result of reduced HIF-1 activity, can easily lead to T cell exhaustion.

Some cancer cells, such as glioblastomas and pancreatic ductal adenocarcinomas, express TDO and IDO1 (or IDO2), and produce LKU (see above). However, tumors in which cancer cells lack IDO1 expression can still trigger upregulation of LKU levels. This can be achieved by stimulating the IFN-γ-dependent upregulation of LKU enzymatic generation through IDO1 in extrahepatic tissues. Another possibility is the TGF-β-dependent activation of IDO1/LKU production in eosinophils, which are present within the TME. Therefore, IDO and the process of enzymatic conversion of L-Trp into LKU should be considered as potential targets for the therapy of a wide range of cancers, where the immune evasion machinery involves LKU.

Materials and methods

Materials

RPMI 1640 and DMEM cell culture media, fetal bovine serum and supplements, and basic laboratory chemicals were obtained from Sigma-Aldrich (Suffolk, UK). Microtiter plates for the Enzyme-Linked Immunosorbent Assay (ELISA) were provided by Oxley Hughes Ltd.

(London, UK). Rabbit antibodies against HIF-1α and AhR were purchased from Abcam (Cambridge, UK). The anti-actin and anti-ARNT antibodies were purchased from Proteintech (Manchester, UK). Goat anti-mouse and anti-rabbit fluorescent dye-labeled antibodies were obtained from Li-COR (Lincoln, Nebraska USA). ELISA-based assay kits/antibodies for the detection of galectin-9, VISTA, IL-2, and TGF-β were purchased from Bio-Techne (R&D Systems, Minneapolis, MN, USA). All other chemicals used were of the highest grade commercially available.

Cell lines and primary human cells/samples

The cell lines employed in this study were purchased from either the European Collection of Cell Cultures, American Tissue Culture Collection, or CLS Cell Lines Service GmbH and were accompanied by identification test certificates. Wilms' tumor cell line WT-3ab was kindly provided by Dr. C. Stock (Children's Cancer Research Institute, Vienna, Austria) and cultured as described previously[30].

Jurkat T cells, MCF-7, WT-3ab, and K562 were cultured in RPMI 1640 medium supplemented with 10% fetal bovine serum, penicillin (50 IU/ml), and streptomycin sulfate (50 µg/ml). LN18 cells were cultured in DMEM media supplemented with 10% fetal bovine serum, penicillin (50 IU/ml), and streptomycin sulfate (50 µg/ml).

Mononuclear-rich leukocytes were isolated from human blood (following ethical approval REC reference: 16-SS-033) using Ficoll-density centrifugation, according to the manufacturer's protocol. Cell numbers were determined using hemocytometers and diluted with HEPES-buffered Tyrode's solution before treatment, as indicated in the text.

NK cells were purified as described previously[24]. Primary human T cells were isolated from PBMCs using a commercial CD3 T cell negative isolation kit (BioLegend), as described before, and resuspended in RPMI 1640 medium supplemented with 10% fetal bovine serum and penicillin/streptomycin mix[2,20].

Human tissue samples

Primary human tumor tissue samples paired together with peripheral tissues (also called "normal" or "healthy" of the same patients) were collected surgically from breast cancer patients treated at the Colchester General Hospital, following informed and written consent taken before surgery. Paired normal (healthy) peripheral tissues were removed by pathologists during the macroscopic examination of a tumor. Blood samples were collected before breast surgery from patients with primary breast cancer, and before treatment from patients with metastatic breast cancer. Samples were also collected from healthy donors (individuals with no diagnosed pathology) and were used as control samples. Blood separation was performed using the buoyancy density method employing Histopaque 1119–1 (Sigma, St. Louis, MO, USA), according to the manufacturer's protocol. Ethical approval documentation for these studies was obtained from the NRES Essex Research Ethics Committee and the Research & Innovation Department of the Colchester Hospitals University, NHS Foundation Trust (MH 363 [AM03] and 09/H0301/37).

Preparation of nuclear extracts

The nuclear extracts were prepared according to a widely used procedure. Briefly, cells were re-suspended in 20 mM Tris buffer (pH 7.5–8.0) containing 100 mM NaCl, 300 mM sucrose, and 3 mM $MgCl_2$ and left on ice for 10 min, and then centrifuged at 4°C at 3,000 rpm for 10 min using an Eppendorf centrifuge. Supernatants containing everything except nuclei were removed. Pellets were re-suspended on ice in 20 mM Tris buffer (pH 8.0), 100 mM NaCl, and 2 mM EDTA and the 4.6 M NaCl was added to bring NaCl to a final concentration of 300 mM. The extracts were then homogenized in a glass homogenizer on ice and left on ice for 30 min, followed by centrifugation at 24,000 × g for 20 min at 4°C. The supernatants were then used for further investigation.

Western blot analysis

HIF-1α protein, AhR, and ARNT were measured by western blotting and compared to β-actin (protein loading control), as previously described[6].

Enzyme-linked immunosorbent assays (ELISAs)

The levels of TGF-β, IFN-γ, VISTA, galectin, and IL-2 were measured in the cell culture medium, human blood plasma, and some of the cell lysates by ELISA using R&D Systems kits (see Materials section) according to the manufacturer's protocols. HMGB1 was measured in human blood plasma using a MyBioSource kit, according to the manufacturer's protocol.

Chromatin Immunoprecipitation (ChIP)

ChIP was performed as described previously[2] on resting LN18 cells and those incubated with 2 ng/ml TGF-β. Cells (5×10^6) were used for immunoprecipitation. Cross-linking was performed using 1.42% formaldehyde, followed by quenching with 125 mM glycine for 5 min. Cells were then washed twice with PBS and subjected to ChIP in accordance with the ChIP-IT high-sensitivity kit (Active Motif) protocol. Immunoprecipitation was performed using mouse monoclonal anti-Smad3 antibody (R&D Systems, Minneapolis, MN, USA). An IgG isotype control antibody was used as a negative control. The Smad3 epitope recognized by this antibody did not overlap with the DNA and co-activator binding sites of this protein. Immunoprecipitated DNA was purified and subjected to quantitative real-time PCR (qRT-PCR) as outlined below. The following primers were designed using the NCBI Primer-BLAST primer design tool: forward, 5'-GGAACGGGCAACTTGGTTTCT-3' and reverse: 5'-TCTAACTGTACCTGACTGCGG-3'. These primers allow amplification of the fragment of the promoter region of the IDO1 gene, which surrounds the Smad3-binding sites.

Analysis of HIF-1 DNA-binding activity

HIF-1 DNA-binding activity was measured by the recently described method[3]. Briefly, 96-well Maxisorp™ microtitre plates were coated with streptavidin and blocked with BSA. A volume of 2 pmol/well biotinylated 2HRE (HRE – hypoxia response element) containing oligonucleotide was immobilized by 1 h incubation at room temperature. The plate was then washed five times with TBST buffer (10 mM Tris-HCl, pH 8.0, 150 mM NaCl, 0.05% Tween-20), followed by 1 h incubation with cell lysate at room temperature. The plate was again washed with TBST buffer and mouse anti-HIF-1α antibody (1:1 000 in TBS with 2% BSA) was added. After 1 h of incubation at room temperature the plate was washed with TBST buffer and then incubated with Li-Cor goat anti-mouse secondary antibody labeled with infrared fluorescent dye. After extensive washing with TBST, the plate was scanned using a Li-Cor fluoroimager.

Analysis of HIF-1α-ARNT and AhR-ARNT interactions

In order to analyze heterodimerisation of HIF-1α or AhR with ARNT into transcription complexes we immunoprecipitated ARNT from the cell lysates using MaxiSorp Nunc plates coated with 1:250 mouse monoclonal anti-ARNT antibody and blocked with BSA. ARNT was immunoprecipitated by 2 h incubation of the whole cell extracts (equal amounts of cellular protein were added to each well) in the coated wells. After extensive washing with TBST, all the proteins which could be bound to ARNT were extracted by adding 0.1 M glycine-HCl buffer. Then these extracts were mixed in the 1:1 ratio with cell lysis buffer used to lyse the cells for Western blot analysis (50 mM Tris pH 7.5, 150 mM NaCl, 5 mM EDTA and 0.5% NP-40) and 4× sample buffer[21]. Samples were then analyzed by Western blot (see above) for HIF-1α and AhR expressions.

Granzyme B activity assays

Granzyme B activity in cell lysates was measured using a fluorometric assay[6] based on the ability of the enzyme to cleave the fluorogenic substrate Ac-IEPD-AFC (Sigma-Aldrich). The in-cell activity of granzyme B (granzyme B catalytic activity in living cells) was measured as described previously[6] by incubating living cells with 150 μM Ac-IEPD-AFC (granzyme B substrate) for 1 h at 37°C in sterile PBS. Total cell fluorescence was measured in living cells using the excitation and emission wavelengths recommended by the Ac-IEPD-AFC manufacturer (Sigma) protocol. An equal number of cells that were not exposed to the granzyme B substrate were used as controls.

qRT-PCR analysis

To detect mRNA levels, qRT-PCR was used qRT-PCR[2,31]. Total RNA was isolated using a GenElute™ mammalian total RNA preparation kit (Sigma-Aldrich) according to the manufacturer's protocol, followed by reverse transcriptase – polymerase chain reaction (RT-PCR) of the target protein mRNA (also performed according to the manufacturer's protocol). This was followed by qRT-PCR analysis. The following primers were used. VEGF: forward – 5'-GTATAAGTCCTGGAGCGT-3,' reverse: 5'-CTCGGAGGGAGTCCCAAA-3'; IDO1: forward – 5'-ACTGTGTCCTGGCAAACTGGAAG-3,' reverse: 5'-AAGCTGCGATTTCCACCAATAGAG-3'; actin: forward – 5′-TGACGGGGTCACCCACACTGTGCCCATCTA-3′; rev erse, 5′-CTAGAAGCATTTGCGGTCGACGATGGAGGG-3. ' Reactions were performed using a LightCycler® 480 qRT-PCR machine and SYBR Green I Master Kit (Roche, Burgess Hill, UK). The assay was performed according to the manufacturer's instructions. Values representing VISTA mRNA levels were normalized against those of β-actin.

Detection of LKU

LKU was measured based on its ability to react with 4-dimethylamino)benzaldehyde. Briefly, we took 160 μL of cell culture medium or blood plasma was added 10 μL 30% (v/v) trichloroacetic acid to each sample, and incubated the samples for 30 min at 50°C in order to hydrolyze N-formylkynurenine to LKU. The samples were then centrifuged at 3000 g for 10 min. 100 μl of supernatants were transferred to wells of a 96-well flat-bottom plate and mixed with 100 μL of freshly prepared Ehrlich's reagent (1.2% w/v 4-dimethylamino)benzaldehyde in glacial acetic acid) followed for 10 min incubation at room temperature. Absorbance was measured using a microplate reader at 492 nm.

TDO/IDO activity measurement (detection of enzymatic generation of N-formylkynurenine)

TDO/IDO activity (or enzymatic conversion of L-Trp into N-formylkynurenine), which was then further converted into LKU, was measured using a previously described method[10] with minor modifications. Briefly, the cell or tissue lysate was added to the reaction mixture containing 50 mM potassium phosphate buffer (pH 6.5), 20 mM ascorbate, 100 μg/mL catalase and 2 mM L-Trp. The reaction was carried out at 37°C for 60 min and terminated by adding 10 μL of 30% (v/v) trichloroacetic acid to 160 μL of sample. Further operations were performed as previously described.

Characterisation of glycolysis and detection of MGO levels

Glycolytic degradation of glucose was analyzed using a colorimetric assay as described previously[21]. Briefly, the assay was performed using cell lysates and the conversion of glucose into lactate in the absence of oxygen (this was achieved by employing an anaerobic chamber). Cell lysates were incubated for 1 h at 37°C with 1% glucose solution in an anaerobic chamber. 2% trichloroacetic acid solution was then used to precipitate proteins. This was followed by carbohydrate precipitation using saturated $CuSO_4$ solution in combination with $Ca(OH)_2$ (at a final concentration of 60 mg/mL). Lactate was then converted into acetaldehyde using concentrated H_2SO_4 at 90°C for 1 min and cooled on ice. Acetaldehyde was detected using the veratrole (1,2-dimethoxybenzene) test. MGO was also detected colorimetrically in the cell culture medium

following biochemical modifications.[21] Briefly, MGO was condensed with reduced GSH (1 mM) for 10 min at 37°C. The complex was then converted into lactate by glyoxalases I and II at pH 8.0 (glyoxalase I converted the complex into D-lactoylglutathione, which was then transformed into lactate by glyoxalase II). Lactate was then measured colorimetrically, as described above.

Cell viability assay

Cell viability was measured using an MTS assay kit (Promega) according to the manufacturer's protocol.

Statistical analysis

Each experiment was performed at least thrice, and statistical analysis was conducted using a two-tailed Student's *t*-test. Multiple comparisons were performed using ANOVA. Post-hoc Bonferroni corrections were applied. The statistical probabilities (p) are expressed as $^{*}p < 0.05$, $^{**}p < 0.01$, and $^{***}p < 0.001$.

Acknowledgments

We thank Diamond Light Source for access to the B23 beamline and funding projects SM24509, SM20755, and SM21202. This work was also supported by the British Society for Immunology (to SS) and Swiss Batzebär grant (to EF-K and SB).

Disclosure statement

No potential conflict of interest was reported by the authors.

Funding

The work was supported by the British Society for Immunology, Diamond Light Source Ltd and Swiss Batzebär grant.

Data availability statement

The data presented in this study are presented in the main and supplementary figures . All the raw data are available from the corresponding author upon request.

References

1. Kyrysyuk O, Wucherpfennig KW. Designing cancer immunotherapies that engage T Cells and NK Cells. Annu Rev Immunol. 2023;41(1):17–38. doi:10.1146/annurev-immunol-101921-044122.
2. Schlichtner S, Yasinska IM, Ruggiero S, Berger SM, Aliu N, Prunk M, Kos J, Meyer NH, Gibbs BF, Fasler-Kan E, et al. ExpressiOn of the immune checkpoint protein VISTA is differentially regulated by the TGF-beta1 - Smad3 signaling pathway in rapidly proliferating human cells and T lymphocytes. Front Med. 2022;9:790995. doi:10.3389/fmed.2022.790995.
3. Selnø ATH, Schlichtner S, Yasinska IM, Sakhnevych SS, Fiedler W, Wellbrock J, Klenova E, Pavlova L, Gibbs BF, Degen M, et al. Transforming growth factor beta type 1 (TGF-beta) and hypoxia-inducible factor 1 (HIF-1) transcription complex as master regulators of the immunosuppressive protein galectin-9 expression in human cancer and embryonic cells. Aging. 2020;12:23478–23496. doi:10.18632/aging.202343.
4. Yang R, Sun L, Li CF, Wang YH, Yao J, Li H, Yan M, Chang WC, Hsu JM, Cha JH, et al. Galectin-9 interacts with PD-1 and TIM-3 to regulate T cell death and is a target for cancer immunotherapy. Nat Commun. 2021;12(1):832. doi: 10.1038/s41467-021-21099-2.
5. Yasinska IM, Gonçalves Silva I, Sakhnevych SS, Ruegg L, Hussain R, Siligardi G, Fiedler W, Wellbrock J, Bardelli M, Varani L, et al. High mobility group box 1 (HMGB1) acts as an "alarmin" to promote acute myeloid leukaemia progression. OncoImmunology. 2018a;7(6):e1438109. doi:10.1080/2162402X.2018.1438109.
6. Yasinska IM, Meyer NH, Schlichtner S, Hussain R, Siligardi G, Casely-Hayford M, Fiedler W, Wellbrock J, Desmet C, Calzolai L, et al. Ligand-receptor interactions of galectin-9 and VISTA suppress human T lymphocyte cytotoxic activity. Front Immunol. 2020;11:580557. doi:10.3389/fimmu.2020.580557.
7. El-Fattah EEA. IDO/Kynurenine pathway in cancer: possible therapeutic approaches. J Transl Med. 2022;20(1):347. doi:10.1186/s12967-022-03554-w.
8. Mezrich JD, Fechner JH, Zhang X, Johnson BP, Burlingham WJ, Bradfield CA. An interaction between kynurenine and the aryl hydrocarbon receptor can generate regulatory T cells. J Immunol. 2010;185(6):3190–3198. doi:10.4049/jimmunol.0903670.
9. Badawy AA-B. Kynurenine pathway of tryptophan metabolism: regulatory and functional aspects. International Journal Of Tryptophan Research. 2017;10:1178646917691938. doi:10.1177/1178646917691938.
10. Zhai L, Ladomersky E, Bell A, Dussold C, Cardoza K, Qian J, Lauing KL, Wainwright DA. Quantification of IDO1 enzyme activity in normal and malignant tissues. Methods Enzymol. 2019;629:235–256.
11. Tan VX, Guillemin GJ. Kynurenine pathway metabolites as biomarkers for amyotrophic lateral sclerosis. Front Neurosci. 2019;13:1013. doi:10.3389/fnins.2019.01013.
12. Sorgdrager FJH, Naude PJW, Kema IP, Nollen EA, Deyn PP. TryptopHan metabolism in inflammaging: from biomarker to therapeutic target. Front Immunol. 2019;10:2565. doi:10.3389/fimmu.2019.02565.
13. Song H, Park H, Kim YS, Kim KD, Lee HK, Cho DH, Yang JW, Hur DY. L-kynurenine-induced apoptosis in human NK cells is mediated by reactive oxygen species. Int Immunopharmacol. 2011;11(8):932–938. doi:10.1016/j.intimp.2011.02.005.
14. Semenza GL. HIF-1 and tumor progression: pathophysiology and therapeutics. Trends Mol Med. 2002;8(4):S62–67. doi:10.1016/S1471-4914(02)02317-1.
15. Ochs K, Ott M, Rauschenbach KJ, Deumelandt K, Sahm F, Opitz CA, von Deimling A, Wick W, Platten M. Tryptophan-2,3-dioxygenase is regulated by prostaglandin E2 in malignant glioma via a positive signaling loop involving prostaglandin E receptor-4. J Neurochem. 2016;136(6):1142–1154. doi:10.1111/jnc.13503.
16. Opitz CA, Litzenburger UM, Opitz U, Sahm F, Ochs K, Lutz C, Wick W, Platten M, Oresic M. The indoleamine-2,3-dioxygenase (IDO) inhibitor 1-methyl-D-tryptophan upregulates IDO1 in human cancer cells. PLoS One. 2011;6(5):e19823. doi:10.1371/journal.pone.0019823.
17. Prokhorov A, Gibbs BF, Bardelli M, Ruegg L, Fasler-Kan E, Varani L, Sumbayev VV. The immune receptor Tim-3 mediates activation of PI3 kinase/mTOR and HIF-1 pathways in human myeloid leukaemia cells. Int J Biochem Cell Biol. 2015;59:11–20. doi:10.1016/j.biocel.2014.11.017.
18. Watcharanurak K, Zang L, Nishikawa M, Yoshinaga K, Yamamoto Y, Takahashi Y, Ando M, Saito K, Watanabe Y, Takakura Y. Effects of upregulated indoleamine 2, 3-dioxygenase 1 by interferon γ gene transfer on interferon γ-mediated antitumor activity. Gene Ther. 2014;21(9):794–801. doi:10.1038/gt.2014.54.
19. Chen W, Frank ME, Jin W, Wahl SM. TGF-beta released by apoptotic T cells contributes to an immunosuppressive milieu. Immunity. 2001;14:715–725. doi:10.1016/S1074-7613(01)00147-9.
20. Schlichtner S, Yasinska IM, Lall GS, Berger SM, Ruggiero S, Cholewa D, Aliu N, Gibbs BF, Fasler-Kan E, Sumbayev VV.

T lymphocytes induce human cancer cells derived from solid malignant tumors to secrete galectin-9 which facilitates immunosuppression in cooperation with other immune checkpoint proteins. J Immunother Cancer. 2023;11. doi:10.1136/jitc-2022-005714.

21. Gonçalves Silva I, Ruegg L, Gibbs BF, Bardelli M, Fruehwirth A, Varani L, Berger SM, Fasler-Kan E, Sumbayev VV. The immune receptor Tim-3 acts as a trafficker in a Tim-3/galectin-9 autocrine loop in human myeloid leukemia cells. Oncoimmunology. 2016;5 (7):e1195535. doi:10.1080/2162402X.2016.1195535.
22. Ala M. The footprint of kynurenine pathway in every cancer: a new target for chemotherapy. Eur J Pharmacol. 2021;896:173921. doi:10.1016/j.ejphar.2021.173921.
23. Newman AC, Falcone M, Huerta Uribe A, Zhang T, Athineos D, Pietzke M, Vazquez A, Blyth K, Maddocks ODK. Immune-regulated IDO1-dependent tryptophan metabolism is source of one-carbon units for pancreatic cancer and stellate cells. Mol Cell. 2021;81:2290–2302 e2297. doi:10.1016/j.molcel.2021.03.019.
24. Gonçalves Silva I, Yasinska IM, Sakhnevych SS, Fiedler W, Wellbrock J, Bardelli M, Varani L, Hussain R, Siligardi G, Ceccone G, et al. The tim-3-galectin-9 secretory pathway is involved in the immune escape of human acute myeloid leukemia cells. EBioMedicine. 2017;22:44–57. doi:10.1016/j.ebiom.2017.07.018.
25. Teo Hansen Selnø A, Schlichtner S, Yasinska IM, Sakhnevych SS, Fiedler W, Wellbrock J, Berger SM, Klenova E, Gibbs BF, Fasler-Kan E, Sumbayev VV. 2021. High Mobility Group Box 1 (HMGB1) induces toll-like receptor 4-mediated production of the immunosuppressive protein galectin-9 in human cancer cells. *Frontiers in Immunology* 12: 675731
26. Yasinska IM, Gonçalves Silva I, Sakhnevych S, Gibbs BF, Raap U, Fasler-Kan E, Sumbayev VV. Biochemical mechanisms implemented by human acute myeloid leukemia cells to suppress host immune surveillance. Cell Mol Immunol. 2018b;15(11):989–991. doi:10.1038/s41423-018-0047-6.
27. Gajanayaka N, Dong SXM, Ali H, Iqbal S, Mookerjee A, Lawton DA, Caballero RE, Cassol E, Cameron DW, Angel JB, et al. TLR-4 agonist induces IFN-gamma production selectively in proinflammatory human M1 macrophages through the PI3K-Mtor- and JNK-MAPK-activated p70S6K pathway. J Immunol. 2021;207:2310–2324. doi:10.4049/jimmunol.2001191.
28. Kraaij MD, Vereyken EJ, Leenen PJ, van den Bosch TP, Rezaee F, Betjes MG, Baan CC, Rowshani AT. Human monocytes produce interferon-gamma upon stimulation with LPS. Cytokine. 2014;67 (1):7–12. doi:10.1016/j.cyto.2014.02.001.
29. Kanevskiy LM, Telford WG, Sapozhnikov AM, Kovalenko EI. Lipopolysaccharide induces IFN-γ production in human NK cells. Front Immunol. 2013;4:11. doi:10.3389/fimmu.2013.00011.
30. Stock C, Ambros IM, Lion T, Zoubek A, Amann G, Gadner H, Ambros PF. Genetic changes of two Wilms tumors with anaplasia and a review of the literature suggesting a marker profile for therapy resistance. Cancer Genet Cytogenet. 2002;135 (2):128–138. doi:10.1016/S0165-4608(01)00647-1.
31. Yasinska IM, Sakhnevych SS, Pavlova L, Teo Hansen Selnø A, Teuscher Abeleira AM, Benlaouer O, Gonçalves Silva I, Mosimann M, Varani L, Bardelli M, et al. ThE tim-3-galectin-9 pathway and its regulatory mechanisms in human breast cancer. Front Immunol. 2019;10:1594. doi:10.3389/fimmu.2019.01594.